25th ABCM International Congress of Mechanical Engineering
October 20-25, 2019, Uberlândia, MG, Brazil

COBEM-2019-0960
RANS SIMULATION OF THE WAVY LEADING EDGE PHENOMENA AT HIGH REYNOLDS NUMBER REGIME

Rafael da Silva Rosário
William Denner Pires Fonseca
School of Mechanical Engineering, University of Campinas, SP - Brazil
rafael.s.rosario@gmail.com
fonsecawdp@gmail.com
Ricardo Galdino da Silva
Institute of Aeronautics and Space, São José dos Campos, SP - Brazil
ri_galdino@yahoo.com.br
Adson Agrico de Paula
Technological Institute of Aeronautics, Department of Aircraft Design, São José dos Campos, SP - Brazil
adson@ita.br

Abstract. *Considering the lack of data on the performance of wavy leading edge airfoils at high Reynolds numbers regime and intending to contribute to this fast growing research topic, the present work aims to provide a numerical investigation on this phenomenon at Reynolds number equal to 3X10^6. We use RANS (Reynolds Average Navier-Stokes) simulations to invest the flow over configuration with and without wavy leading edge at high Reynolds. We use an infinite wing formed by NACA 0021 profile as baseline geometry. The wavy leading edge has an amplitude equal to 3% of mean aerodynamic chord and a wavelength equal to 11% of mean aerodynamic chord. Initially, studies for the validation of numeric parameters such as turbulence model and computational mesh were performed and compared with literature data. We analyze the pressure distribution, the shear stress lines on the wing surface, and aerodynamics coefficients to achieve a better understanding of the flow features. The comparisons between the straight leading edge and the wavy leading edge showed that the second generated the higher maximum lift coefficient. The present results also suggest that, at an angle of attack near the stall, the configuration with wavy leading edge generates a drag coefficient bigger than the straight leading edge.*

Keywords: *Wavy Leading Edge, CFD Analysis, RANS Simulation*

1. INTRODUCTION

Flow control devices have allowed meaningful changes in aircraft design in the past decades. In particular, researches have studied passive flow control devices extensively. The motivation involves a potential gain in hydrodynamic and aerodynamic performance for engineering designs such as aircraft wings, control surfaces, propellers, fans, wind turbines, and automotive airfoils. Usually, researches find inspiration by simply observing how Nature works. In that sense, the observation of humpback whales flipper patterns (Fig. 1) brought to light an interest in the wavy leading edge phenomena.

Figure 1: Humpback whale flipper patterns (http://elelur.com/mammals/humpback-whale.html)

Despite its large size, the humpback whale is agile when it is maneuvering and swimming with its flippers at high angles of attack. For the first time, Bushnell and Moore (1991) suggested that the presence of tubercles (wavy leading edge) on the flippers play an essential role on the maneuvering capability of the humpback whales, in particular when it is feeding.

Motivated by the tubercles function of the humpback flipper, Watts and Fish (2001) carried out studies of the sinusoidal leading edge. That showed a potential gain in aerodynamic and hydrodynamic efficiency. These simulations were realized using an airfoil NACA 63021 with finite-span (aspect ratio = 2.04) with the panels method and an inviscid flow at large Reynolds number. At an angle of attack 10 degrees, the wavy shape incorporated at leading edge increases 4.8% in the lift, decreases 10.9% in the induced drag, and increases in the lift to drag ratio by 17.6%. The wavy leading edge enhances wing performance at modest angles of attack while offering no detrimental effects at zero angles of attack. However, for a viscous calculation form drag increases 11% at $\alpha = 10^{\circ}$.

The first experimental study of the wavy leading edge was carried out by Miklosovic *et al.* (2004), who built a scale model of a flipper using a NACA 0020 airfoil in wind tunnel testing, in which the Reynolds number ranges from 505,000 to 520,000. The tests showed promising results with an increase of 40% on the stall angle and 6% in the maximum lift, and a decrease of 32% in the drag on the post-stall regime when it compared to smooth flipper model. At a low angle of attack, both models showed similar results. Moreover, the scalloped flipper showed better lift to drag ratio (L/D). As consequence, it is able to achieve higher performance at all angle of attack except $10^{\circ} < \alpha < 12^{\circ}$. They conclude that specifically scalloped leading edge of flipper has the function of delaying stall by providing higher lift at a higher angle of attack. The results of Miklosovic *et al.* (2004) were motivators for later studies in the wavy leading edge phenomenon (Johari *et al.*, 2007; Stanway, 2008; Chen *et al.*, 2012; Natarajan *et al.*, 2014).

There are many potential applications for wavy leading edge, especially at the at low Reynolds numbers regime. One of those is UAVs (Unmanned aerial vehicle). That kind of aircraft has small chord length and fly at a relatively low speed, which means operating in low Reynolds number. The maximum lift coefficient reduces because of separation, which appears as a consequence of low Reynolds numbers. As a result, one expected a degeneration on landing performance. Studies indicate that tubercles can reduce the minimum stall-speed without much increase in drag. Furthermore, helicopter and wind turbine blades could also benefit from wavy leading edge incorporation. Those often operate at high angles of attack and therefore subject to dynamic stall, these shapes could have smooth stall behavior and consequently reduced fatigue with the addition of tubercles (Hansen, 2012).

Paula (2016) provides an extensive experimental study at low Reynolds number and applications, including boat rudders, missile fins, and aircraft control surfaces, all of which could benefit from performance advantage. Increasing aerodynamic performance of control surfaces could lead to smaller sized surfaces and reduced weight.

Xingwei *et al.* (2013) conducted numerical simulation with a RANS (Reynolds-averaged Navier-Stokes) formulation to evaluate the changes on the flow due to tubercles, which are present at the leading edge of a NACA 63021 airfoil. The results show that the tubercles generate vortex in the troughs in the chord-wise direction, which increase the velocity downstream of the tubercle peak. Locally, it increases the flow restitence to an adverse pressure gradient. Thus, the flow separation in this region delayed, and it concentrated at the trailing edge. Whereas in the troughs region, the flow separation seems to anticipate. This work brings to us, the idea of moment exchange between peaks and troughs of the airfoil as a flow control mechanism through vortex generation.

Favier *et al.* (2012) conducted another computational study at Reynolds number equal to 800. This simulation shows that vortex originate from both sides of the tubercles peaks in a counter-rotating manner, which form a Kelvin-Helmholtz instability. Skillen *et al.* (2014) andRostamzadeh *et al.* (2013) observed similar behavior on CFD (Computational Fluid Dynamics) simulation at a higher Reynolds Number. Those studies use a stalled NACA 0021 airfoil at 20 degrees incidence angle with LES (Large Eddy Simulation) turbulence formulation at Reynolds number equal to 120,000. They also observed the Kelvin-Helmholtz instabilities, which forms at the peaks of the tubercles.Skillen *et al.* (2014) found out another flow mechanism present in such simulation, in which a strong pressure gradient in the spanwise direction causes a secondary flow for a configuration with a wavy trailing edge. This secondary flow contributes to boundary layer re-energizing, which would delay separation.

Since the humpback whale swims at a low Reynolds number and low Mach number, it is natural that the researches developed studies at such a flow regime.Bolzon *et al.* (2015) suggest that there is also a potential benefit of the application of for high Mach number. In this case, one would be able to reduce the wave drag by inducing the wavy leading edge.

In this context, the present effort intends to analyze the flow topology and aerodynamic coefficients of the airfoil NACA 0021 with and without a wavy leading edge. We define the amplitude equal to 3% of the mean aerodynamic chord and the wavelength equal to 11% of the mean aerodynamic chord to design the wavy leading edge. We use a commercial CFD code, ANSYS FLUENT, to do all the simulations at Reynolds number equal to 3 million.

2. THEORICAL FORMULATION

The present study aims to characterize the problem of airfoils with a wavy leading edge with the RANS turbulence models. In this section, a theoretical formulation of the Reynolds Averaged Navier-Stokes (RANS) equation and also the theoretical formulations of two turbulence models (k-epsilon and Sparlart-Allmaras) are presented.

2.1 RANS equations

The RANS equations can be written in cartesian coordinates for a two-dimensional and incompressible flow as:

$$\frac{\partial \mathtt{U}}{\partial x} + \frac{\partial \mathtt{V}}{\partial y} = 0 \tag{1}$$

$$\frac{\partial \mathtt{U}}{\partial t} + \mathtt{div(UU)} = -\frac{1}{\rho}\frac{\partial P}{\partial x} + \nu \mathtt{div}(\mathtt{grad}(U)) + \frac{1}{\rho}\left[\frac{\partial(-\rho\overline{u^2})}{\partial x} + \frac{\partial(-\rho\overline{u'v'})}{\partial y} + \frac{\partial(-\rho\overline{u'w'})}{\partial z}\right] \tag{2}$$

$$\frac{\partial \mathtt{V}}{\partial t} + \mathtt{div(VU)} = -\frac{1}{\rho}\frac{\partial P}{\partial y} + \nu \mathtt{div}(\mathtt{grad}(V)) + \frac{1}{\rho}\left[\frac{\partial(-\rho\overline{u'v'})}{\partial x} + \frac{\partial(-\rho\overline{v'^2})}{\partial y} + \frac{\partial(-\rho\overline{v'w'})}{\partial z}\right] \tag{3}$$

Here, ν is the kinetic viscosity, U and V are the velocities that can be defined using the Reynolds decomposition as:

$$\mathtt{U} = \overline{\mathtt{u}} + u' \tag{4}$$

$$\mathtt{V} = \overline{\mathtt{v}} + v' \tag{5}$$

Where the terms $\overline{u}$ and $\overline{v}$ are the means of velocity in the directions x and y, respectively and u' and v' are the fluctuations.

In Eqs. (2) and (3) the terms dependent on the last portion are called Reynolds stresses. These are composed of two normal stresses and two shear stresses. The normal stresses involve the respective variances of the x and y velocity fluctuations. They are always non-zero because they contain squared velocity fluctuations. The shear stresses contain second moments associated with correlations between different velocity components. A correlation between pairs of different velocity components due to the structure of the vortical eddies ensures that the turbulent shear stresses are also non-zero and usually very large compared with the viscous stresses in a turbulent flow. The equation set presented is called the Reynolds averaged Navier–Stokes equations (Versteeg and Malalasekera, 2007).

2.2 Turbulence closure

For the closure of the equations, we use the turbulence models $k-\epsilon$ and Sparlart Allmaras. The model k-ϵ, proposed by Lauder and Sharma (1974); Launder and Spalding (1983), consists in the use of the conservation equations of dissipation of turbulent kinetics energy, according to Eqs. (6) and (7).

$$\frac{\partial(\rho k)}{\partial t} + \mathtt{div}(\rho k \mathbf{U}) = \mathtt{div}\left[\frac{\mu_t}{\sigma_k}\mathtt{grad}(k)\right] + 2\mu_t S_{ij}.S_{ij} - \rho\epsilon \tag{6}$$

$$\frac{\partial(\rho \epsilon)}{\partial t} + \mathtt{div}(\rho \epsilon \mathbf{U}) = \mathtt{div}\left[\frac{\mu_t}{\sigma_\epsilon}\mathtt{grad}(\epsilon)\right] + C_{1\epsilon}\frac{\epsilon}{k}2\mu_t S_{ij}.S_{ij} - C_{2\epsilon}\rho\frac{\epsilon^2}{k} \tag{7}$$

In this equations σ_k, σ_ϵ, $C_{1\epsilon}$ and $C_{2\epsilon}$ are constants. Where σ_k and σ_ϵ are Prandtl numbers connecting the diffusivity of k and ϵ to the eddy viscosity μ_t.

The Sparlart Allmaras model consist of one transport equation for kinematic eddy viscosity parameter $\tilde{v}$.(Spalart and Allmaras, 1992) proposed this turbulence model. The transport equation for $\tilde{v}$ is as follows:

$$\frac{\partial(\rho\tilde{v})}{\partial t} + \mathtt{div}(\rho\tilde{v}\mathbf{U}) = \frac{1}{\sigma_v}\mathtt{div}\left[(\mu + \rho\tilde{v})\mathtt{grad}(\tilde{v}) + C_{b2}\rho\frac{\partial\tilde{v}}{\partial x_k}\frac{\partial\tilde{v}}{\partial x_k}\right] + C_{b1}\rho\tilde{v}\tilde{\Omega} - C_{w1}\rho\left(\frac{\tilde{v}}{\kappa y}\right)^2 f_w \tag{8}$$

3. NUMERICAL METHODOLOGY

3.1 Solution method, geometries and mesh

The spatial discretization of the equations set presented above was performed using the finite volume method and an implicit approach was used for temporal discretization. As for the solution of the pressure-velocity coupling and the nonlinearities present in the set of equations, a scheme of a segregated nature was chosen, more precisely by SIMPLE (Semi Implicit Linked Equations), for the gradient, was chosen the least-squares cell-based and for the others terms, the second-order upwind method was set. Commercial ANSYS FLUENT software was employed for all numerical predictions on a NACA 0021 airfoil with straight leading edge and wavy leading edge. Fig. 2 shows the geometries of the airfoils.

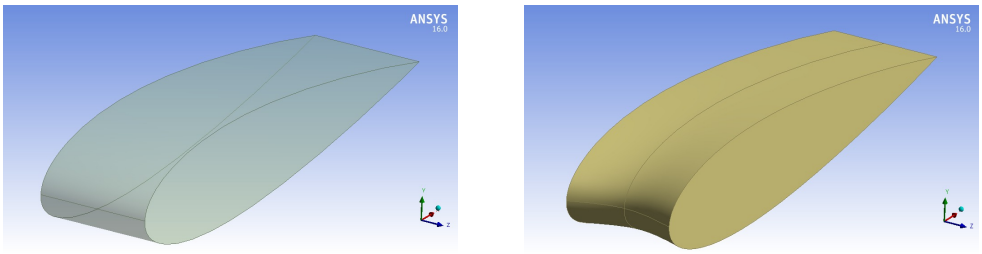

(a) straight leading edge airfoil (b) wavy leading edge airfoil

Figure 2: Geometries studied

As the present work seeks to evaluate the aerodynamic characteristics in high Reynolds, we performed a study on the RANS turbulence models, $k - \epsilon$ and Sparlart Allmaras (Fig. 3) and we compared those results with results extracted from Rocha *et al.* (2018) and Xfoil code. From this study, we verified that Sparlart Allmaras model presents better. Thus, we chose the Sparlart-Allmaras turbulence model as the model that we will use on the rest of the present effort.

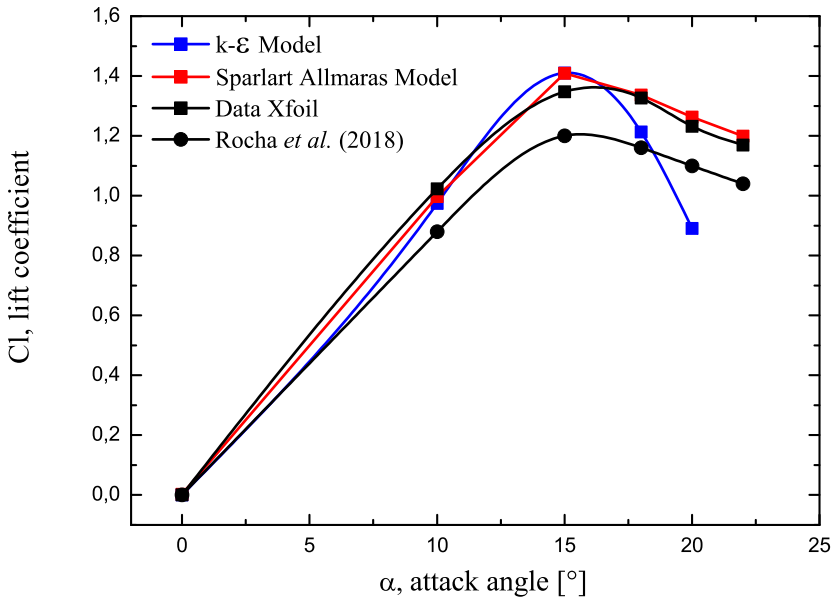

Figure 3: Lit curve for turbulence model verification

We developed a structured mesh, which for this case is a C-type domain. The $y^+ \approx 1$, which require a mesh refinement near the airfoil surface. We also refine the wake region, as shown in Fig. 4. To improve the accuracy of our simulations, we smooth the size variation of the cells. Based on the structure of the mesh described, we carry out a refinement study, in which we use a mesh with 1420000 cells (coarse mesh), 2288000 cells (medium mesh) and 3104000 (fine mesh) cells. From this study, we observed that the difference between the medium mesh and fine mesh was lower than 3% (Figs. 5 and 6). Therefore, we constructed a mesh similar to the medium mesh (Fig. 4) for the wavy profile configuration.

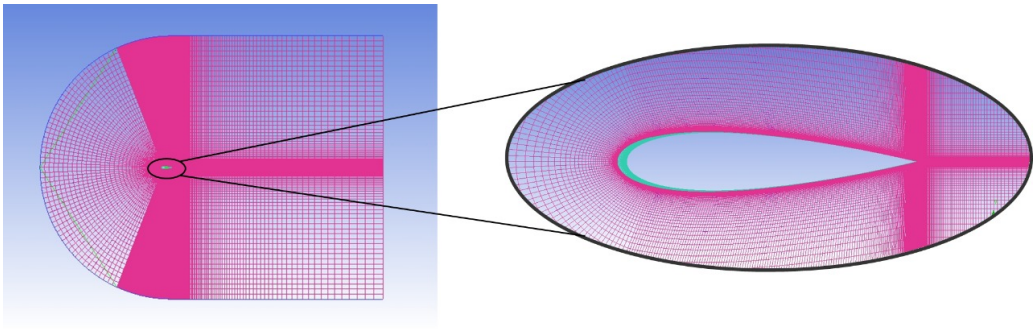

Figure 4: Computational mesh

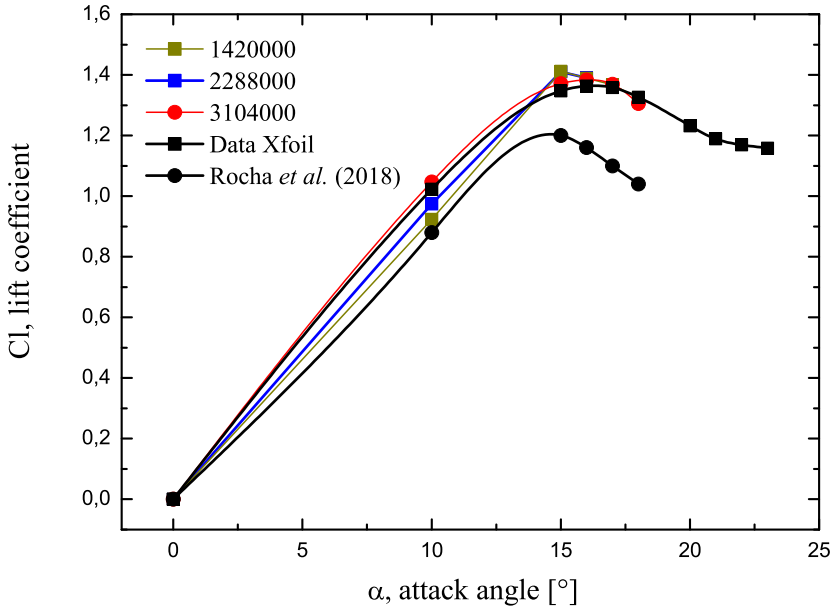

Figure 5: Lift curve for the mesh independence test

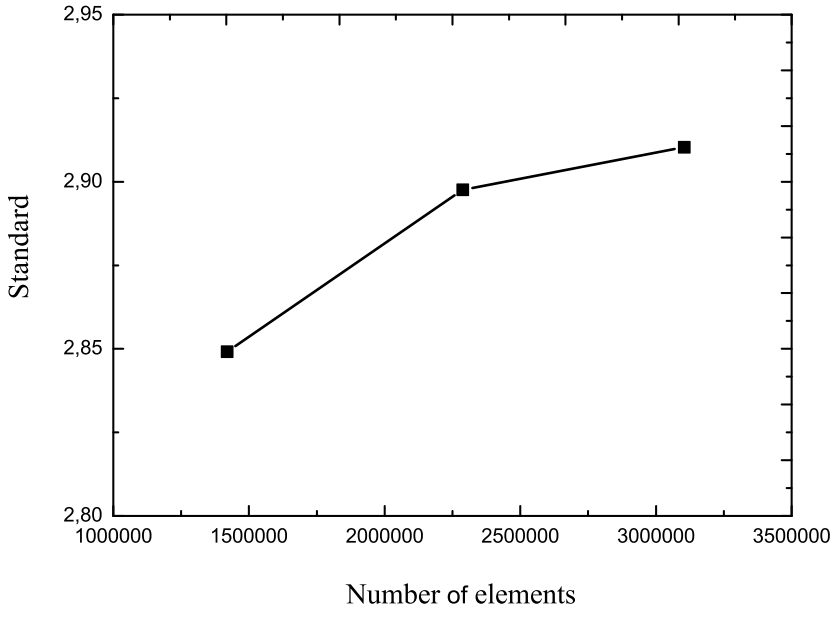

Figure 6: Convergence study of mesh

As already mentioned, we defined the simulation flow conditions to reproduce the experimental procedures, such conditions were Reynolds number equal to $3X10^6$, Mach number equal to 0.2697, temperature equal to 298 K, reference pressure equal to 101325 Pa, density equal to 1.185 kg/m^3 and the viscosity equal to $1.836X10^{-5}$ kg/m.s. The distance from the airfoil surface to the far-field boundary surface corresponds to 12.5 times the mean aerodynamic chord. The wetted area for the straight leading edge configuration is equal 0.0539 m^2 and for the wavy leading edge configuration is equal to 0.0531 m^2.

3.2 Boundary conditions

Uniform velocity is applied at the inlet, with zero freestream turbulence. Lateral boundaries are modeled as slip walls. At the outlet, an atmosphere pressure condition is employed, whereas periodicity is applied in the spanwise direction. The wing surface is modeled as a nonslip wall, which means zero surface velocity, and a zero gradient condition in the wall-normal direction for the surface pressure. No special treatment is required at the wall, since the grid is sufficiently fine to fully resolve the boundary layer, and the dynamic subgrid model gives the correct asymptotic behavior approaching a solid surface without the need for damping functions (Germano *et al.*, 1991).

4. RESULTS AND DISCUSSION

The complexity of the flow resulting from the presence of WLE (Wavy Leading Edge) studied in the present work is analyzed through the pressure and velocity fields, shear stress lines and lift, drag and pressure coefficients. As presented in experimental works, for moderate to high Reynolds number flow regimes, for example, in Mattos *et al.* (2016) and Rocha *et al.* (2018), there is an increase in the maximum lift coefficient by 7.83 % concerning SLE (Straight Leading Edge), as can be seen in Fig. 7. Regarding the drag (Fig. 8), It's possible to verify for $\alpha < 5°$, the airfoil with WLE have coefficients in the same order as was shown by the SLE, however near the stall (α =15°), WLE have a drag coefficient 31.1% greater than SLE. This increase of the drag coefficient in the airfoil with WLE for high angles of attack is due to the fact of re-circulation of the flow in the valleys of the wavy leading.

It is noted from Fig. 7 that such a flow control device (WLE) contributes for a greater maximum lift coefficient, this phenomena can be credited by the WLE modification of the flow topology. The Figs. 9 and 10 exhibit the pressure fields topology in the pre-stall regime (15, 17 and 18°), for SLE and WLE, respectively. It is observed that the change of geometry produces an adverse pressure gradient in a direction not parallel to the flow generating vortex parallel in the surface of the airfoil. This adverse pressure gradient increases the intensity of the shear stress (Figs. 11 and 12) who is responsible for the reduction and stabilization of the recirculation region, and thus the lift enhancement. Thus, the low inertia boundary layer fluid that is transported away by a secondary flow is replaced by higher momentum fluid, drawn from above. This reenergizes the boundary layer behind each chord peak, delaying separation.

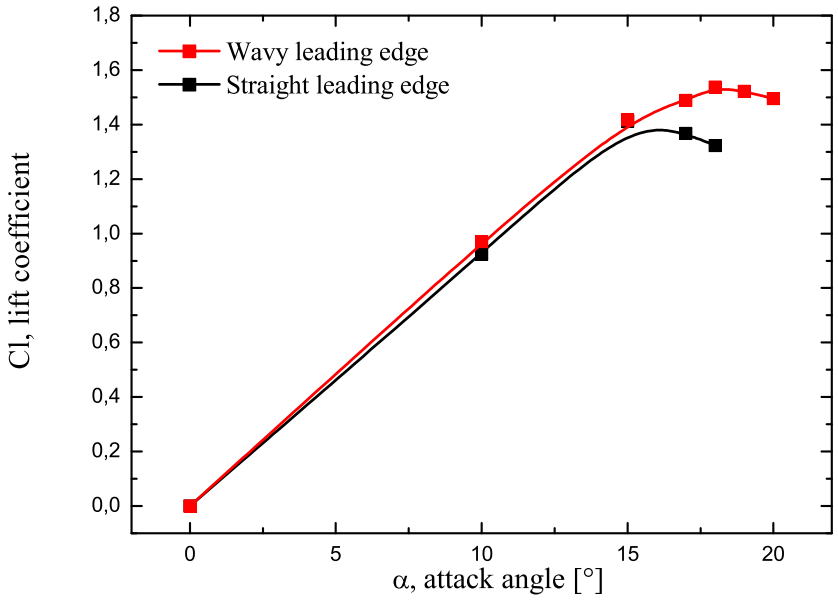

Figure 7: Comparision Cl vs. α for SLE and WLE configurations

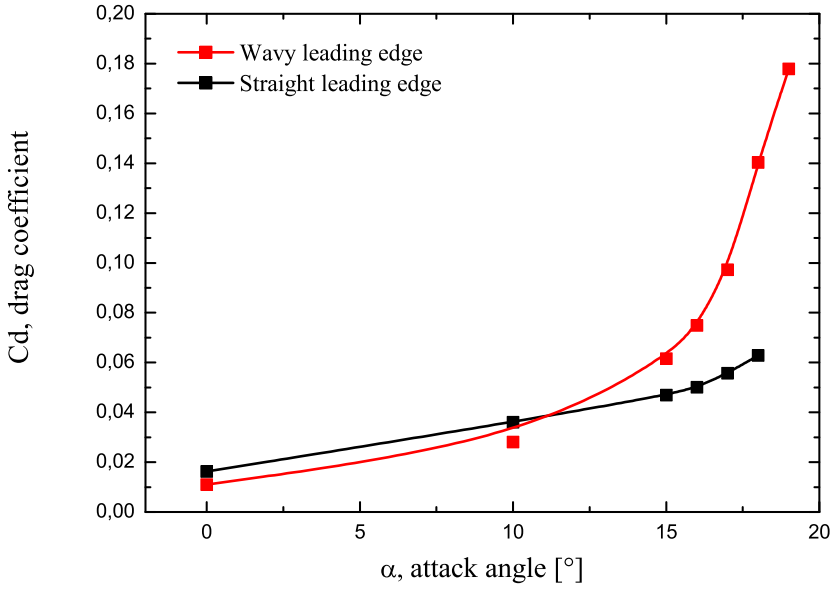

Figure 8: Comparision Cd vs. α for SLE and WLE configurations

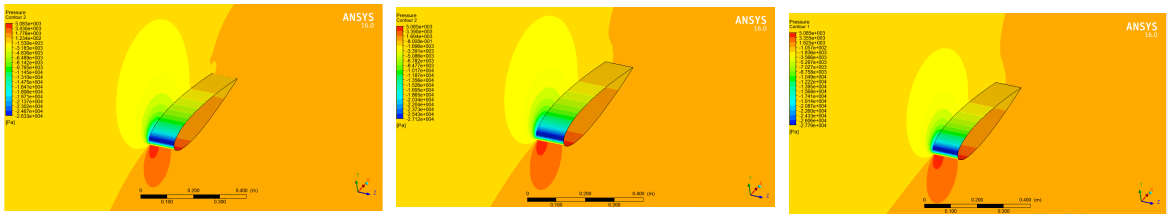

(a) α = 15° (b) α = 17° (c) α = 18°

Figure 9: Pressure fields for the straight leading edge airfoil

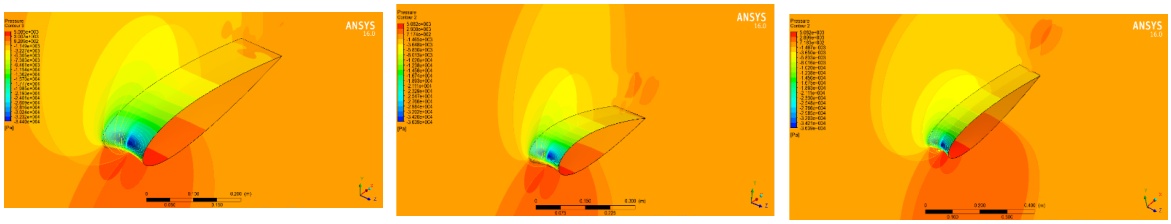

(a) α = 15° (b) α = 17° (c) α = 18°

Figure 10: Pressure fields for the wavy leading edge airfoil

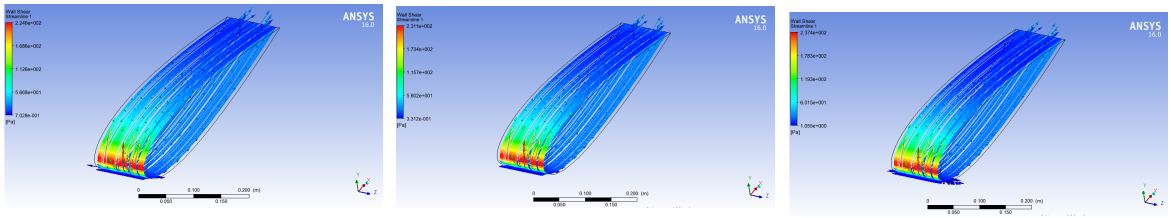

(a) α = 15° (b) α = 17° (c) α = 18°

Figure 11: Wall shear for the straight leading edge airfoil

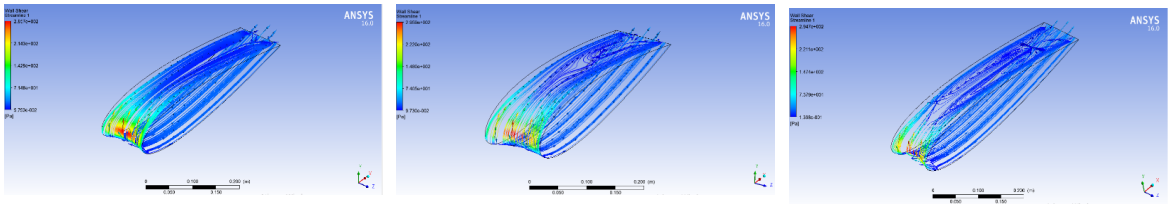

(a) α = 15° (b) α = 17° (c) α = 18°

Figure 12: Wall shear for the wavy leading edge airfoil

Also can be observed when both pressure coefficient charts are compared to angles of attack 15, 17 e 18° (Figs. 13, 14 and 15, respectively) the initial part of the wavy profile, for angles above 15°, has a higher value of negative pressure, which can delay the point of separation of the flow and, consequently, delaying the stall by 3 degrees. from this observation, and considering that the lift coefficient can be calculated by the integral of the pressure coefficient, we conclude that the increase of cl of the WLE concerning STE is due to this phenomenon.

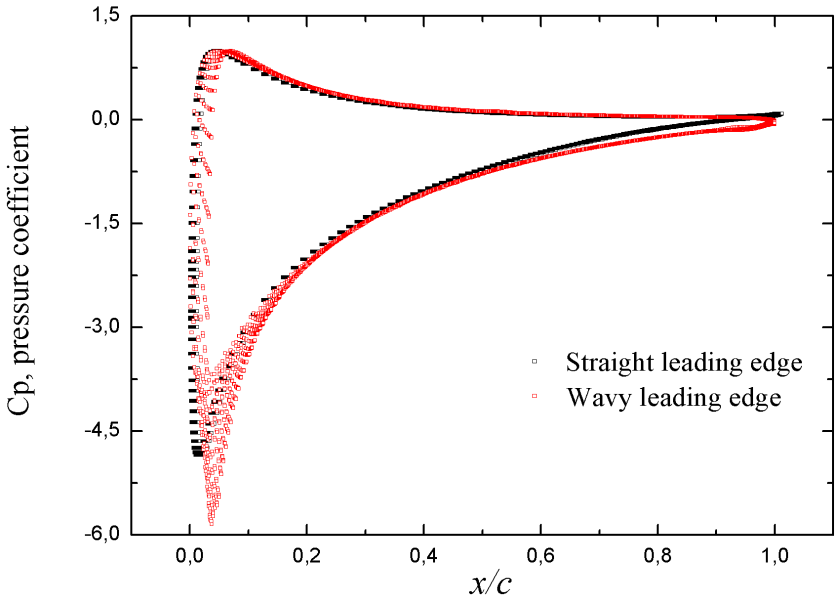

Figure 13: Comparison Cp vs. x/c for SLE and WLE configurations. α = 15°

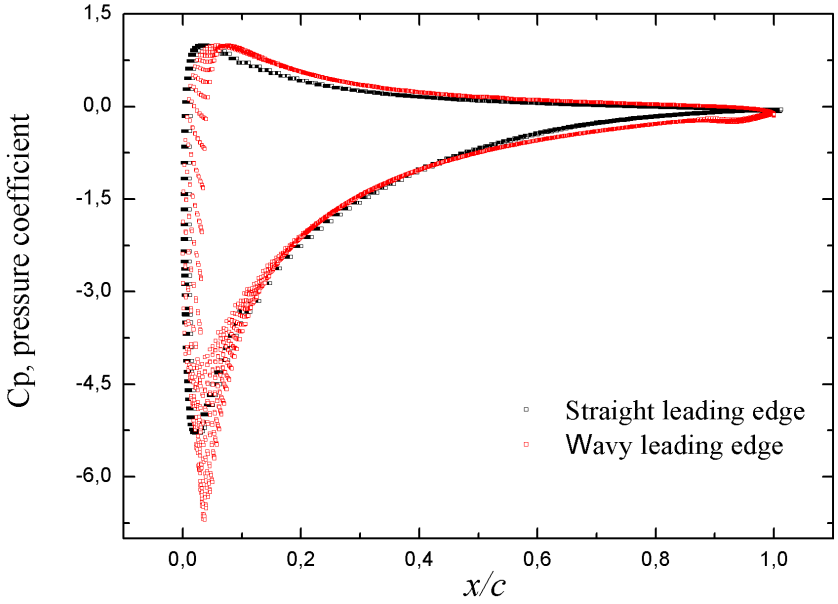

Figure 14: Comparison Cp vs. x/c for SLE and WLE configurations. α = 17°

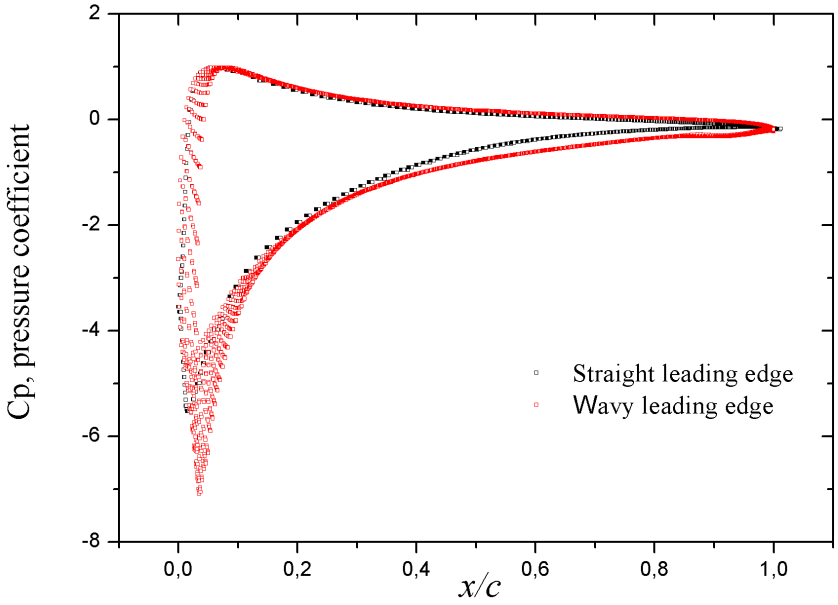

Figure 15: Comparison Cp vs. x/c for SLE and WLE configurations. α = 18°

5. CONCLUSIONS

RANS simulations are used for studying the effects of a tubercled leading edge in a high Reynolds Regime over a NACA 0021 infinite wing. In the present work, two models configurations are tested on the flow regime, an SLE model of the NACA 0021 and another with WLE (3% of the aerodynamic chord and the period of 11% of this). From the results it was concluded that the presence of WLE contributes to a maximum lift value greater than SLE, however, a considerable increase in the drag coefficient also occurs.

As far as this work could check, these flow control devices in the configurations of amplitude and wavelength studies contribute to better lift values at the expense of a considerable increase in drag. Figures 9 to 12 present perceptions about the effects of flow topology on the WLE condition. It is believed that the energy extracted from the vortices, generated from the oscillation of the flow, seems to be distributed to separate regions and, therefore, may be responsible for the replacement of the flow in the boundary layer. However, as the simulations were solved using a RANS methodology, it is difficult to analyze the smaller scales of turbulence to have more precise conclusions. Therefore, more numerical tests, with DES (Detached Eddy Simulation) and LES (Large eddy simulation) approaches, will be realized for a better understanding of the WLE phenomena.

6. ACKNOWLEDGEMENTS

The authors are grateful for the support of CNPq (National Council for Scientific and Technological Development) and ITA (Technological Institute of Aeronautics), for the scholarship granted to the first author and for the infrastructure made available for conducting research, respectively.

7. REFERENCES

Bolzon, M.D., Kelso, R.M. and Arjomandi, M., 2015. "Tubercles and their applications". *Journal of Aerospace Engineering*, Vol. 29, No. 1, p. 04015013.

Bushnell, D.M. and Moore, K., 1991. "Drag reduction in nature". *Annual review of fluid mechanics*, Vol. 23, No. 1, pp. 65–79.

Chen, J., Li, S. and Nguyen, V., 2012. "The effect of leading edge protuberances on the performance of small aspect ratio foils". In *15th International Symposium on Flow Visualization*. pp. 25–28.

Favier, J., Pinelli, A. and Piomelli, U., 2012. "Control of the separated flow around an airfoil using a wavy leading edge inspired by humpback whale flippers". *Comptes Rendus Mecanique*, Vol. 340, No. 1-2, pp. 107–114.

Germano, M., Piomelli, U., Moin, P. and Cabot, W.H., 1991. "A dynamic subgrid-scale eddy viscosity model". *Physics of Fluids A: Fluid Dynamics*, Vol. 3, No. 7, pp. 1760–1765.

Hansen, K.L., 2012. *Effect of leading edge tubercles on airfoil performance.* Ph.D. thesis.

Johari, H., Henoch, C.W., Custodio, D. and Levshin, A., 2007. "Effects of leading-edge protuberances on airfoil performance". *AIAA journal*, Vol. 45, No. 11, pp. 2634–2642.

Lauder, B. and Sharma, B., 1974. "Application of the energy-dissipation model of turbulence to the calculation of flow near a spinning disc". *Letters in Heat and Mass Transfer*, Vol. 1, No. 2, pp. 131–138.

Launder, B.E. and Spalding, D.B., 1983. "The numerical computation of turbulent flows". In *Numerical prediction of flow, heat transfer, turbulence and combustion*, Elsevier, pp. 96–116.

Mattos, B.D., Meneghini, J., Padilha, B.R. and de Paula, A.A., 2016. "The airfoil thickness effect on wavy leading edge performance". In *54th AIAA Aerospace Sciences Meeting*. p. 1306.

Miklosovic, D., Murray, M., Howle, L. and Fish, F., 2004. "Leading-edge tubercles delay stall on humpback whale (megaptera novaeangliae) flippers". *Physics of fluids*, Vol. 16, No. 5, pp. L39–L42.

Natarajan, K., Sudhakar, S. and Paulpandian, S., 2014. "Experimental studies on the effect of leading edge tubercles on laminar separation bubble". In *52nd Aerospace Sciences Meeting*. p. 1279.

Paula, A.A.d., 2016. *The airfoil thickness effects on wavy leading edge phenomena at low Reynolds number regime.* Ph.D. thesis, Universidade de São Paulo.

Rocha, F.A., de Paula, A.A., Sousa, M.d., Cavalieri, A.V. and Kleine, V.G., 2018. "Lift enhancement by wavy leading edges at reynolds numbers between 700,000 and 3,000,000". In *2018 Applied Aerodynamics Conference*. p. 3816.

Rostamzadeh, N., Kelso, R., Dally, B. and Hansen, K., 2013. "The effect of undulating leading-edge modifications on naca 0021 airfoil characteristics". *Physics of fluids*, Vol. 25, No. 11, p. 117101.

Skillen, A., Revell, A., Pinelli, A., Piomelli, U. and Favier, J., 2014. "Flow over a wing with leading-edge undulations". *Aiaa Journal*, Vol. 53, No. 2, pp. 464–472.

Spalart, P. and Allmaras, S., 1992. "A one-equation turbulence model for aerodynamic flows". In *30th aerospace sciences meeting and exhibit*. p. 439.

Stanway, M.J., 2008. *Hydrodynamic effects of leading-edge tubercles on control surfaces and in flapping foil propulsion*. Ph.D. thesis, Massachusetts Institute of Technology.

Versteeg, H.K. and Malalasekera, W., 2007. *An introduction to computational fluid dynamics: the finite volume method*. Pearson education.

Watts, P. and Fish, F.E., 2001. "The influence of passive, leading edge tubercles on wing performance". In *Proc. Twelfth Intl. Symp. Unmanned Untethered Submers. Technol.* Auton. Undersea Syst. Inst. Durham New Hampshire.

Xingwei, Z., Chaoying, Z., Tao, Z. and Wenying, J., 2013. "Numerical study on effect of leading-edge tubercles". *Aircraft Engineering and Aerospace Technology*, Vol. 85, No. 4, pp. 247–257.

8. RESPONSIBILITY NOTICE

The authors are the only responsible for the printed material included in this paper.